Boundary Layers in Planes of Symmetry, Part I: Experiments in Turbulent Flow

V.C. Patel* and J.H. Baek†
University of Iowa, Iowa City, Iowa

Experiments were conducted in the turbulent boundary layer in the windward and leeward planes of symmetry of an axisymmetric body at an incidence of 15 deg. The measurements include pressure distribution, mean velocities, and turbulence. The results are used to assess the influence of external-flow convergence and/or divergence on the turbulence and the overall development of the boundary layer. These data, and the somewhat limited information available from previous experiments, are utilized in Part II[1] of this paper, which describes a complementary computational study to explore further the effects of external-flow convergence and divergence in laminar and turbulent boundary layers.

I. Introduction

THE boundary layer along a plane of symmetry is considered. For three-dimensional bodies, such as ship hulls and aircraft fuselages, the flow in the plane of symmetry provides the boundary conditions to be satisfied by the flow on either side of it and consequently dictates the behavior of the boundary layer over the entire body. The complexity of the plane-of-symmetry boundary layer is intermediate to that of the idealized two-dimensional boundary layer, on the one hand, and the fully three-dimensional boundary layer, on the other. It differs from the former in the presence of lateral flow convergence or divergence and from the latter in the absence of a cross flow. It is of interest to study this rather special boundary layer for several reasons. First, its development can be calculated independently of the flow elsewhere on the body, and therefore the results can be used to provide the boundary conditions for the calculation of the three-dimensional boundary layer on the body. Alternatively, the independent calculations can be used to provide a check on the performance of methods which include the planes of symmetry in the solution procedure. Second, the plane-of-symmetry boundary layer offers the opportunity to isolate and study the influence of flow convergence and divergence in the absence of a cross flow. Divergence of flow out of a plane of symmetry retards the boundary-layer growth and therefore delays transition. Calculations and experiments, however, indicate that prolonged convergence of the external streamlines leads to a zone of divergent flow near the surface, and this provides a mechanism for a vortex type of separation on the body. Third, the turbulent boundary layer in a plane of symmetry provides a simple but effective test of the ability of turbulence models to account for the extra straining of turbulence due to mean-flow convergence and divergence. Fourth, since measurements in nominally two-dimensional boundary layers are usually made in the plane of symmetry of models and ducts of finite, and often small, aspect ratio, such data usually contain undocumented influence of convergence or divergence.

Very few experimental or theoretical studies explicitly devoted to plane-of-symmetry boundary layers have been reported. For laminar flow, Wang [2,3] carried out systematic calculations of boundary-layer development in the symmetry plane of a prolate spheroid at various incidences and showed that the solutions admit a variety of separation patterns on the body although the issues of definition and prediction of separation still remain unsettled. Similar calculations have been reported recently by Schneider.[4] Experimental information in laminar flow is rather limited and, as will be discussed later, comes from the measurements of Meier, Kreplin, and others [5-8] on a spheroid at incidence. In turbulent flow, experiments in three-dimensional boundary layers involving planes of symmetry have been carried out by Hornung and Joubert,[9] East and Hoxey,[10] Dechow and Felsch,[11] Krogstad,[12] and Pierce and McAllister.[13] All these considered the boundary layer ahead of a symmetrical obstacle mounted on a flat surface so that the flow in the plane of symmetry is divergent throughout and separates (with zero skin friction) at a saddle point in wall streamlines just ahead of the obstacle. Measurements in the boundary layer along ship keels, and the body of revolution experiments of Meier, Kreplin, and others, and of Ramaprian, Patel, and Choi,[14] also provide some data in the plane of symmetry. However, turbulence measurements were not made in these experiments, and therefore the information necessary to validate turbulence models is not available. Calculations of turbulent boundary layers using integral and differential methods have been reported by many authors, but comparisons with experiments are limited to the mean flow and, in most instances, to planes of symmetry with flow divergence.

From the foregoing brief review, it is clear that data on plane-of-symmetry boundary layers subjected to mean-flow convergence, or simultaneous convergence and divergence, is quite limited, and practically no information is available on the influence of either convergence or divergence on the turbulence. Extensive previous work in nominally two-dimensional boundary layers has indicated a very strong influence of extra rates of strain (in addition to the primary strain rate) due, for example, to surface curvature, rotation, and buoyancy (see Bradshaw[15]) on the turbulence structure. Similar extra strain rates are present in the plane-of-symmetry boundary layer due to the mean-flow convergence and divergence. Turbulence measurements in these flows are therefore of fundamental interest in the study of turbulent shear flow, in general, and three-dimensional boundary layers, in particular.

A body of revolution at incidence is perhaps the simplest configuration that can be used to study all aspects of plane-of-symmetry boundary layers. The potential-flow streamlines (outside the boundary layer) diverge out of the windward plane of symmetry and converge into the leeward plane. Thus, the boundary layer on the windward plane is subjected to a divergent external flow. The convergence of the external

Received Dec. 30, 1985.

*Professor of Mechanical Engineering, Iowa Institute of Hydraulic Research. Member AIAA.

†Research Assistant, University of Iowa; presently at Korea Advanced Institute of Science and Technology, Seoul, Korea.

streamlines into the leward plane initially subjects the flow in the entire boundary layer to convergence but, further downstream, the boundary layer experiences divergence near the wall and convergence in the outer part. The flow in the plane of symmetry of bodies at incidence is therefore the focus of the present study. However, the results and conclusions are of more general interest.

Mean-flow and turbulence measurements have been made in the boundary layer on the windward and leeward planes of symmetry of a body of revolution that consists of a hemispheric nose joined to a half-spheroid. This first part of the paper is concerned with the experimental study. The results of these experiments, together with those from some previous experiments, are then used in Part II,[1] in conjunction with a boundary-layer calculation method, to illustrate the influence of external-flow convergence and divergence on laminar, transitional, and turbulent boundary layers.

II. Experimental Arrangement and Procedures

The experiments were conducted in the 5-ft octagonal-section wind tunnel of the Iowa Institute of Hydraulic Research with the same model as that used in the previous three-dimensional mean-flow experiments of Ref. 14. The model was mounted at a nominal incidence of 15 deg, and the measurements were made at a tunnel speed $Q_0 = 21.4$ m/s, so that the Reynolds number based on model length L was 1.86×10^6.

Figure 1 shows the model geometry and the notation used in the presentation of the data. X is the distance measured along the model axis from the nose. The measurements were made in the orthogonal coordinates (x,y,θ); x and y being along and normal to the surface, respectively, and $\theta = 0$ and 180 deg corresponding to the windward and leeward generators, respectively. The mean and fluctuating velocity components in the (x,y,θ) directions are denoted by (U,V,W) and (u,v,w). All data are normalized using L and Q_0.

Since the surface pressure distribution and mean-velocity profiles had been measured in the previous experiments, these could have been supplemented simply by making the corresponding turbulence measurements. However, in order to obtain a complete and self-consistent set of data, it was decided to repeat the previous measurements. Small but systematic differences between the new and previous data were observed. Although the reasons for these are not entirely clear, it is believed that they may be due to small differences in the model alignment or the effectiveness of the trip wire located at $X/L = 0.04$, used to promote transition. Only the new data are reported here.

The experimental procedures used for the measurement of the pressure distribution on the body and the mean-velocity profiles by pitot probes were similar to those described in Ref. 14. Although a simple pitot tube would have sufficed for the measurement of mean velocity in the plane of symmetry, a three-hole yaw probe was used in order to ascertain the degree of flow symmetry and to measure the variation of static pressure across the boundary layer.

Standard x-type (DISA 55P51) hot-wire probes were employed for the turbulence measurements. The difficulty of making reliable turbulence measurements in a three-dimensional flow (by multiple probes, triple wires, or laser anemometers) is well known. However, measurements in the plane of symmetry can be made with some confidence using conventional cross-wire probes due to the absence of a cross flow. Thus, these data serve the additional purpose of providing a check on measurements made elsewhere on the body by other means. The anemometer voltages were processed digitally by using a Preston A-D converter and the HP-1000 computer. Measurements were made with the plane containing the x wires normal to the body surface (u-v configuration) and parallel to the surface (u-w configuration) to obtain all velocity components.

The experimental results consist of 1) pressure distributions measured by surface taps and the yaw probe; 2) distributions of the mean-velocity components U and W measured by the yaw probe, and U,V, and W by hot wires; 3) the Reynolds stresses $\overline{u^2}$, $\overline{v^2}$, $\overline{w^2}$, $\overline{uv}$, and $\overline{uw}$; and 4) the triple products $\overline{u^3}$, $\overline{uv^2}$, $\overline{u^2v}$, $\overline{v^3}$, $\overline{w^3}$, $\overline{uw^2}$ and $\overline{u^2w}$. It should be mentioned that some of these quantities should be zero in the plane of symmetry, and therefore the data can be used to ascertain the degree of symmetry realized in the experiment. The yaw-probe data were obtained at six stations labeled 1-6: $X/L = 0.169$, 0.234, 0.326, 0.419, 0.530, and 0.641 but, because of the limitations of the traverse mechanism inside the model and the differences in probe lengths, hot-wire data could be obtained at only four intermediate stations labeled $3H$-$6H$: $X/L = 0.291$, 0.384, 0.495, and 0.606 (see Fig. 1). The uncertainties in the data have been estimated to be as follows: 0.5% of freestream dynamic head for surface pressures; 0.5 deg in angle, 0.7% of dynamic head in velocity magnitude, and 1.5% of dynamic head in local pressure for yaw-probe measurements; and 0.6% of freestream velocity for all hot-wire data, resulting in uncertainties of the order of 10% in the Reynolds stresses.

III. Pressure Distribution

Figure 2 shows the pressure distributions on the body along the windward and leeward planes of symmetry. The pressure coefficient C_p is defined by

$$C_p = (P - P_0)/\tfrac{1}{2}\rho\, Q_0^2$$

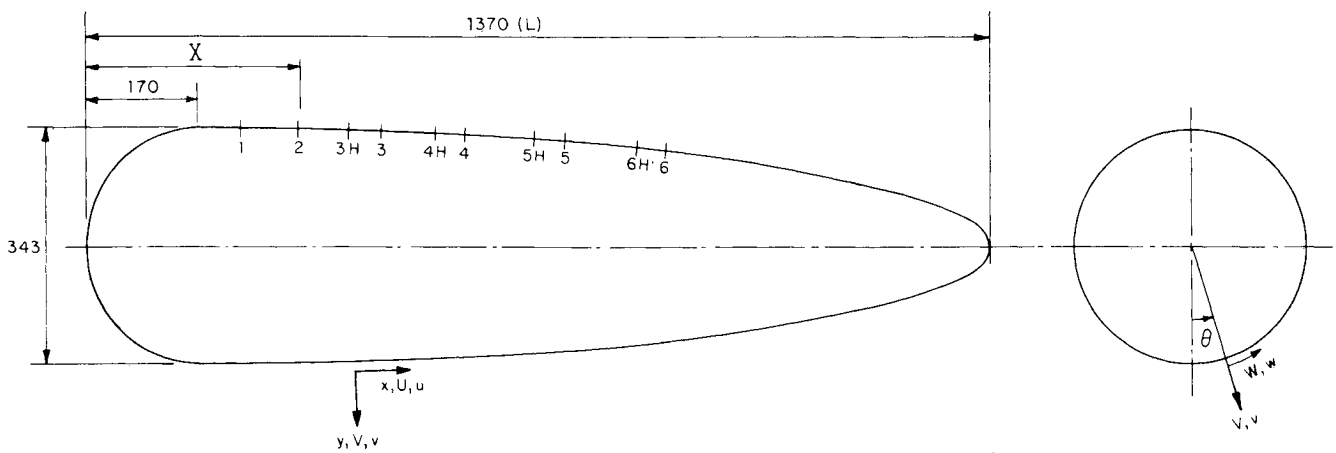

Fig. 1 Model geometry, measurement stations (in mm), and coordinates.

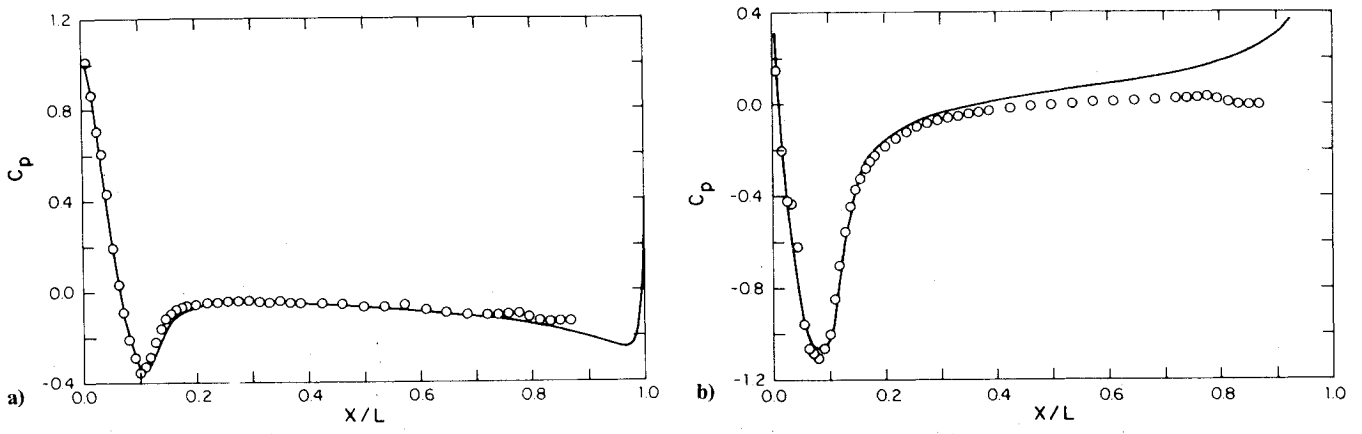

Fig. 2 Surface pressure distribution at 15-deg incidence. o, experiment; —, potential flow: a) windward and b) leeward.

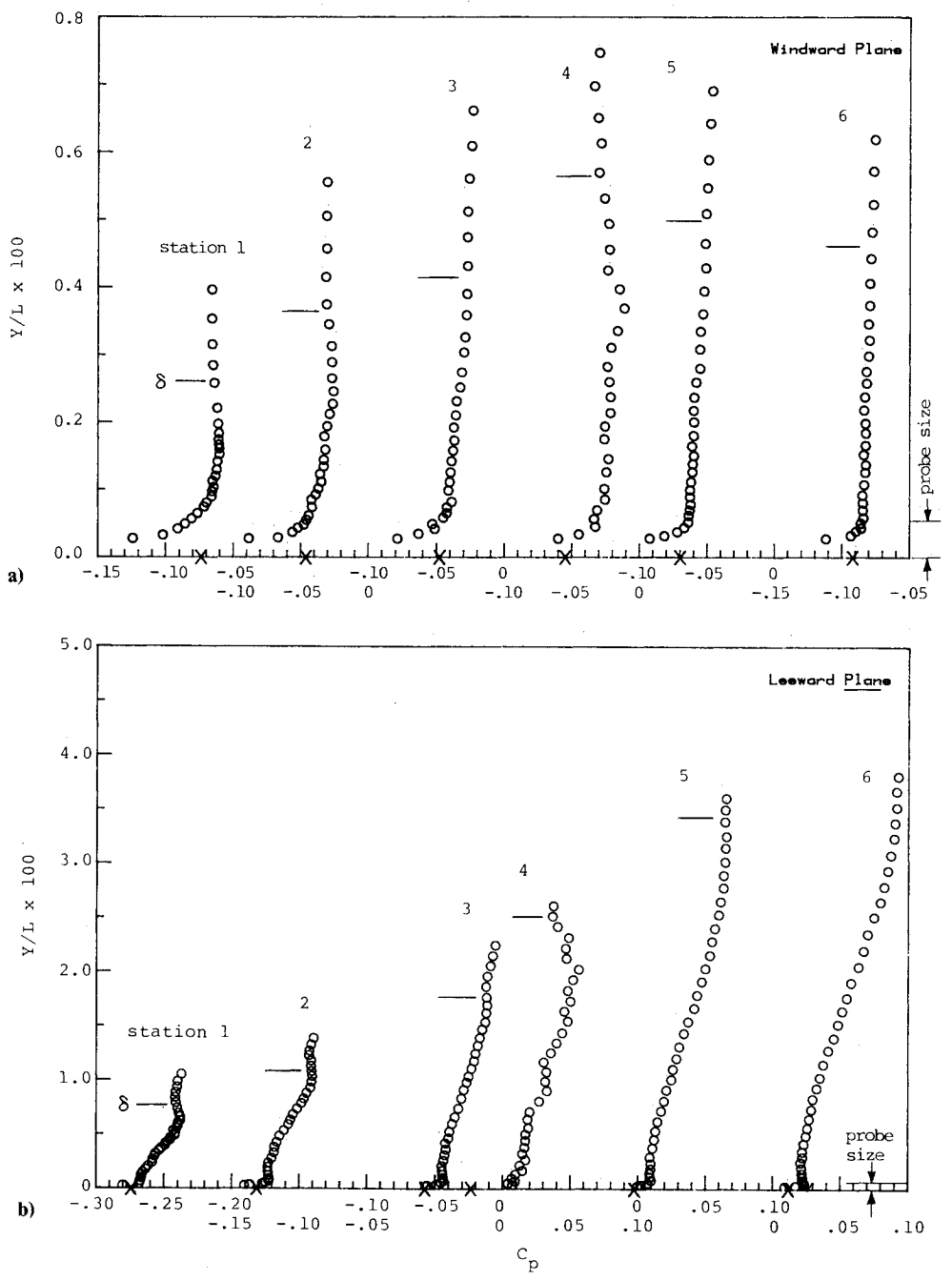

Fig. 3 Pressure profiles; o, yaw probe; x, surface tap: a) windward and b) leeward.

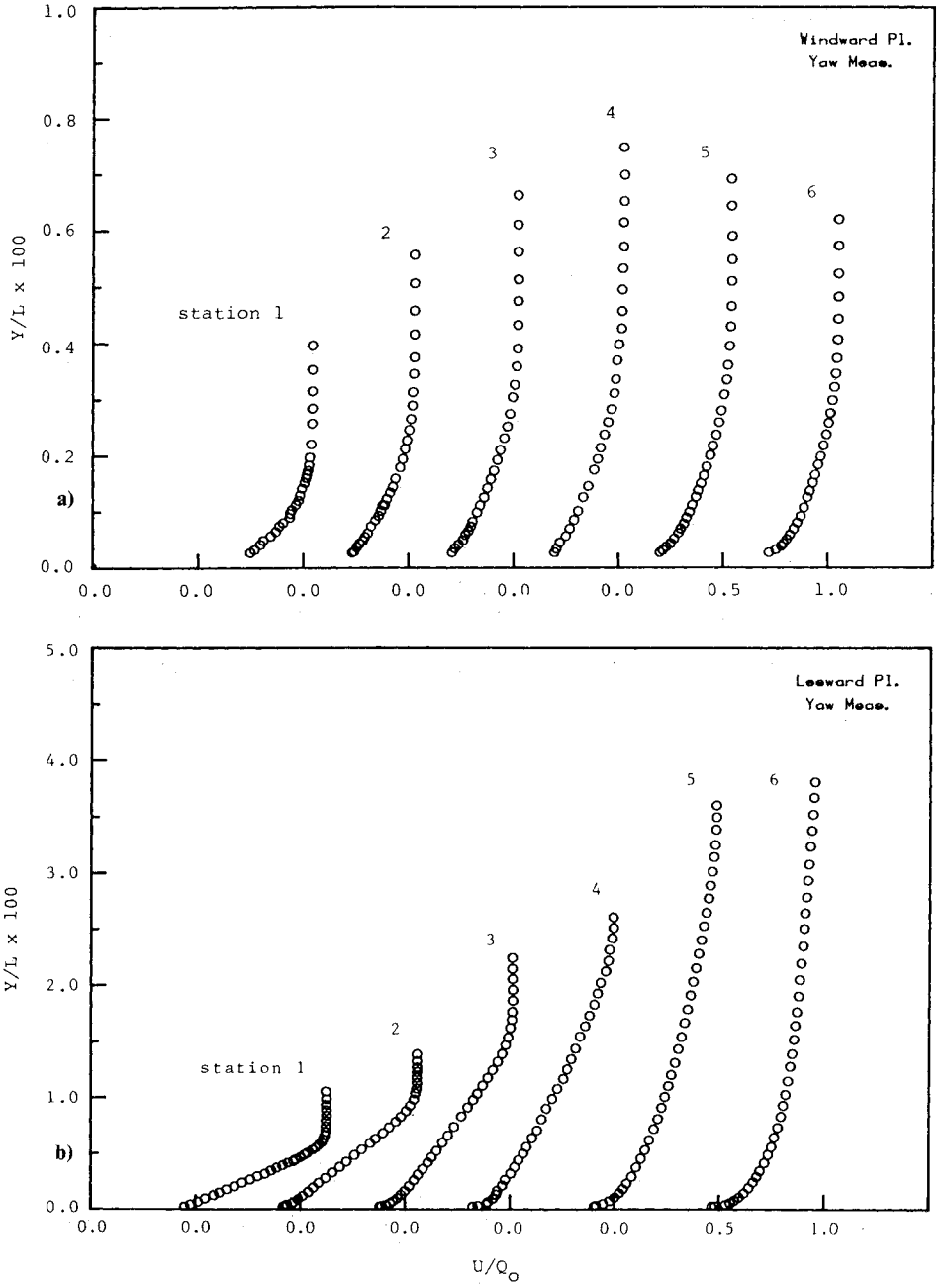

Fig. 4 Mean-velocity profiles measured by yaw probe: a) windward and b) leeward.

where P is the local pressure; P_0 and Q_0 are the pressure and velocity, respectively, in the undisturbed stream in the tunnel; and ρ is density. The measurements are compared with the potential-flow distribution calculated by the method of Landweber and Macagno[16] at an incidence of 15 deg. The general agreement between the data and theory over the front of the body suggests that tunnel blockage is negligible and that the departures observed for $X/L > 0.8$ on the windward side and $X/L > 0.3$ on the leeward side are due to viscous-inviscid interaction.

The variations of pressure across the boundary layer measured by the yaw probe at the six axial stations are shown in Fig. 3. Also indicated, is the size of the probe, the local boundary-layer thickness δ determined from the total-pressure profiles, and the independently measured surface pressures. The data point closest to the wall thus corresponds to the reading at the probe center with the probe resting on the wall. It is clear that the data-points within distances of the order of one probe-height show rather peculiar trends, presumably resulting from interference between the wall and the probe. This is particularly noticeable on the windward side, where the boundary layer is rather thin. If these data are disregarded, it is seen that the pressures measured at the wall agree reasonably well with extrapolations from those measured further away within the boundary layer.

In general, the variation of pressure across the thin boundary layer on the windward side is quite small ($\Delta C_p < 0.02$), and the pressure increase through the layer is consistent with the convex streamwise curvature of the body surface. On the leeside, the pressure is also seen to increase with distance from the wall at all stations, with the largest increase (of the order of 0.07 in C_p) observed at the last measurement station, but the convex surface curvature is not large enough to account for this. Thus, the observed pressure variation on the leeside must be attributed to viscous-inviscid interaction. It is interesting to note that the differences between the pressures measured at the wall and at the edge of the boundary layer are almost identical to the differences between the measured and potential-flow surface pressure distributions shown in Fig. 2. Thus, it would appear that the potential-flow solution provides a good approximation to the flow outside the boundary layer. This is confirmed by the velocity measurements presented later.

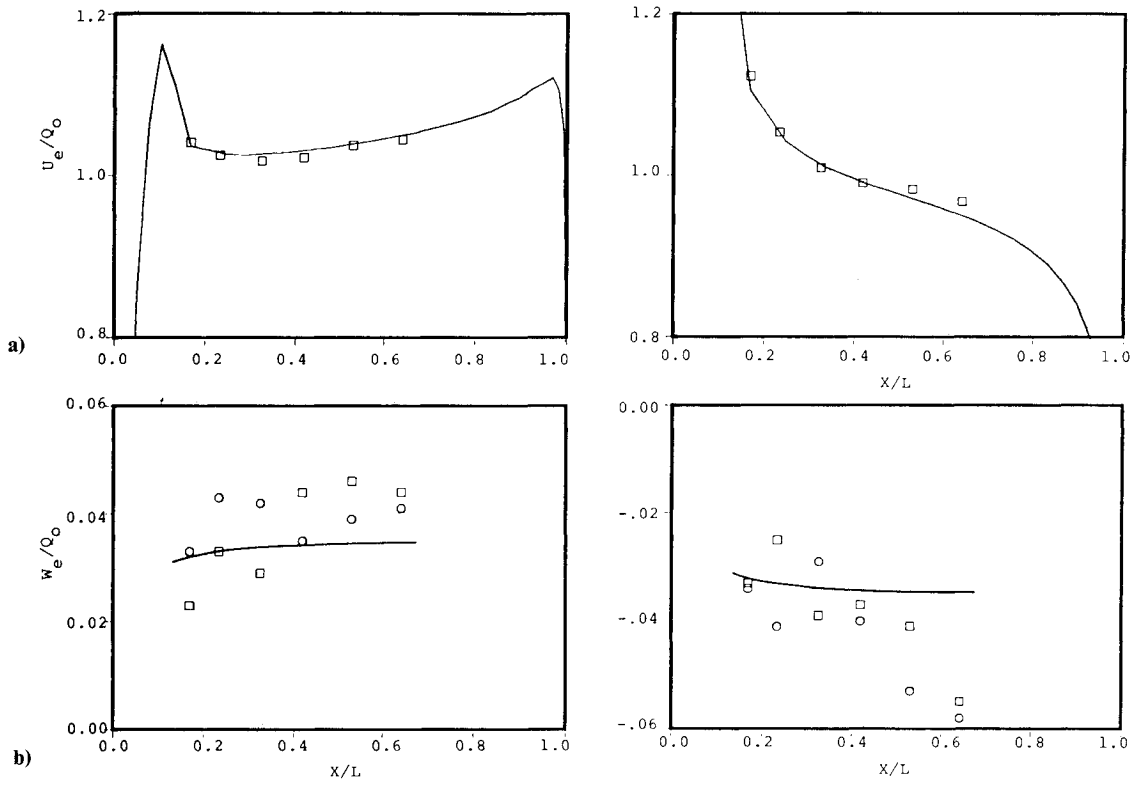

Fig. 5 Velocity at the edge of the boundary layer: U_e on symmetry plane; W_e at 4 deg on either side of symmetry plane. □, ○, experiment; —, potential flow: a) windward and b) leeward.

IV. Mean Velocity Profiles

The component of velocity W in the circumferential direction should be zero in the plane of symmetry. The yaw-probe measurements indicated that the angle between the velocity vector and the geometric plane of symmetry of the body was nowhere greater than 3 deg, i.e., $W \leq 0.05U$. This was also confirmed by the hot-wire measurements. Although $W=0$, its circumferential gradient, $\partial W/\partial\theta$, is not zero. In fact, this quantity is a measure of the rate of lateral convergence or divergence of the mean flow from either side of the symmetry plane. Initially, an effort was made to measure this by using the yaw probe along body generators on either side of the symmetry plane. However, reliable data could not be obtained because of the rather small cross-flow angles and the accuracy with such data could be differentiated to obtain the required gradient.

The velocity profiles measured by the yaw probe are shown in Fig. 4. It is clear that the boundary layer on the windward side remains thin (less than 8.2 mm in the region of measurements) as a result of flow divergence out of this plane, and indeed the thickness decreases beyond station 4. On the other hand, the boundary layer on the leeside is much thicker, due to the convergence of flow into this plane, and exhibits a large growth rate. These features are of course the same as those noted in Ref. 14.

The measured longitudinal variation of the velocity at the edge of the boundary layer U_e is compared with that deduced from the potential-flow pressure distribution in Fig. 5. As noted earlier, the agreement is seen to be quite satisfactory. Also shown in this figure are the measured circumferential velocities W_e along generators 4 deg on either side of the symmetry planes. The scatter in the data and the magnitudes involved clearly illustrate the difficulty of accurately measuring the rates of convergence and divergence even in the external flow. Nevertheless, these measurements confirm that the experimental flow was reasonably symmetric along the windward and leeward sides. The comparisons with the potential-flow solutions, however, indicate that the actual rates of convergence and divergence are larger than those predicted by potential theory, particularly on the leeside.

All three components of mean velocity, namely, $U, V,$ and $W,$ were also measured with cross wires in two configurations at the four axial stations indicated in Fig. 1. With regard to the hot-wire measurements, we note that the thin boundary layer on the windward side precluded measurements in the inner half of the boundary layer. Also, at station 6H on the leeside, the boundary layer was too thick to be measured in a single traverse of the probe. These measurements were therefore carried out in two parts after carefully realigning the probe and ensuring a region of overlap between the two traverses. From the data presented later, it will be seen that reasonable continuous profiles were obtained in spite of the separate traverses.

The U components measured with the two configurations of cross wires were found to be in excellent agreement. Also, when interpolated, these data showed excellent agreement with the yaw-probe results. The measurements of the W component confirmed the earlier observation that the maximum deviation of the velocity vector from the plane of symmetry was less than 3 deg. The normal velocity component V was found to be small and negative everywhere on the windward side, as would be expected in a thin boundary layer with a laterally divergent flow. In view of these observations, most of the mean-flow data from the hot wires are not presented here. However, the measurements of the normal velocity on the leeside are particularly interesting and are shown in Fig. 6. It is seen that V is positive at the first station (3H), as would be expected from the flow convergence into this plane. Further downstream, beyond station 4H, there is a growing region of negative V near the surface and a region of positive V in the outer part. The former is associated with the development of divergent flow in the inner part of the boundary layer. Thus, the boundary layer along the leeside is initially subjected to convergence, but it experiences simultaneous convergence and divergence further downstream.

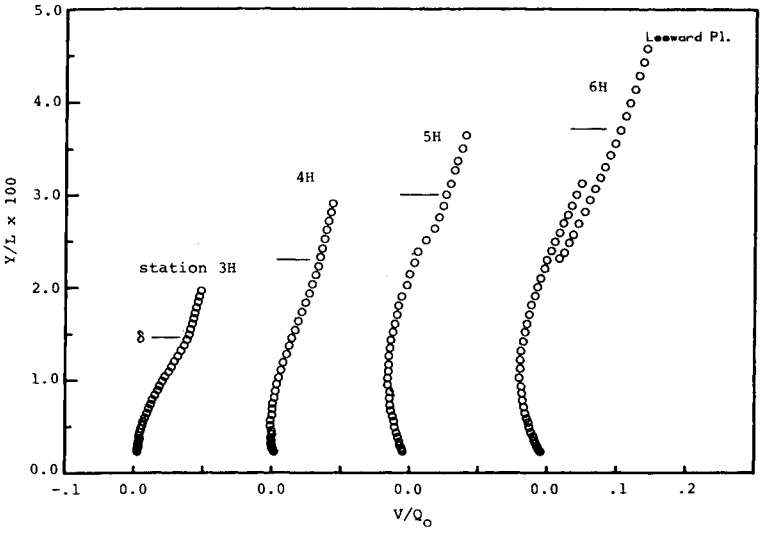

Fig. 6 Normal (V) component of velocity on leeward plane (x-wire data).

V. Turbulence Measurements

Although the hot-wire data were obtained at four longitudinal stations along each plane of symmetry, for the purposes of the present discussion, it is sufficient to show the results at the most upstream (3H) and the most downstream (6H) stations since they contain all the important effects of convergence and divergence. Readers interested in the complete data set should consult Ref. 17. Tabulated data are also available form the authors.

The rms turbulence intensities u', v', and w', defined by $u' = (\overline{u^2})^{1/2}$, etc., are shown in Fig. 7. It is seen that the value of u' measured with the two configurations of the cross wire are in very good agreement, especially in the region where the boundary layer is thick enough for probe-size effects to be negligible. On the windward side, v' and w' are nearly equal and somewhat smaller than u'. It is not clear whether this is significant since data in the important wall region could not be obtained. On the leeside, the relative magnitudes of the three components and the shapes of the distributions at the upstream station are similar to those observed in a two-dimensional boundary layer. However, at the downstream station (6H), major changes appear, both in the shape and relative magnitudes of the three components, and the absolute values are greatly decreased.

The two shear stresses ($\overline{uv}$ and $\overline{uw}$) that were measured are shown in Fig. 8. Note that $\overline{uw}$ should be zero on the plane of symmetry. The third stress, $\overline{vw}$, which was not measured, should also be zero. It is seen that $\overline{uw}$ does not vanish everywhere. The values on the windward side are quite significant although they are all much smaller than the primary stress $\overline{uv}$ in the region of the measurements. The results indicate that $\overline{uw}$ decreases toward the wall whereas $\overline{uv}$ increases continuously. Although the lack of data over a large region in the inner part of the boundary layer precludes any definitive conclusion, the most probable reasons for the nonzero values of $\overline{uw}$ are the effects of probe interference and alignment rather than lack of flow symmetry. On the leeward side, the boundary layer is much thicker, and therefore the same probe enabled measurements to be made closer to the wall, in terms of boundary-layer thickness. In this case, the decrease in $\overline{uw}$ in the near-wall region is clearly seen and, at station 6H, it is practically zero throughout the boundary layer.

The distributions of the primary shear stress $\overline{uv}$ suffer from similar defects on the windward side but are much more complete on the leeside. The values of the wall shear stress, determined independently from the mean-velocity profiles and the law of the wall, are also indicated. It is seen that the measured distributions of $\overline{uv}$ can be extrapolated smoothly (with some uncertainty on the windward side) to the wall shear-stress values, and the resulting slopes of the stress distribution in the wall region are compatible with the local pressure gradients, which can be seen from Fig. 2. Thus, for example, on the leeside, the increase in the Reynolds stress with wall distance at station 3H is indicative of the adverse pressure gradient seen in Fig. 2 at that station, while the nearly constant values at station 6H reflect the small local pressure gradients.

Finally, from Figs. 7 and 8, we note that the general shapes of all Reynolds stress profiles are similar to those expected in two-dimensional boundary layers everywhere except at station 6H on the leeside. The profiles at these stations indicate inflection points in the outer part of the boundary layer that are not observed in two-dimensional flows.

The hot-wire data were processed to determine some commonly used quantities in turbulence models. The distributions of the turbulent kinetic energy $k = (\overline{u^2} + \overline{v^2} + \overline{w^2})/2$ are shown in Fig. 9. Since the normal stresses were measured at different physical locations in the boundary layer by separate traverses, and $\overline{u^2}$ was measured twice, k was determined by taking an average value for $\overline{u^2}$ and interpolations in the other data. Little can be said about these distributions except to note that the turbulence levels at station 6H on the leeside are considerably smaller than those expected in a two-dimensional boundary layer under similar pressure-gradient conditions. These data are presented here to facilitate comparison with calculations by means of turbulence models that use the turbulent kinetic-energy equation.

The so-called structure parameter $a_1 = -\overline{uv}/k$, which is known to demonstrate a degree of universality in turbulent shear flows, was also calculated. A commonly accepted value for a_1 is 0.3. It was found that the data on the windward side indicated values somewhat larger than 0.3, while those on the leeside indicated smaller values. In both cases, the values decreased with downstream distance, but a clear correlation with the mean-flow divergence on the windward side, and convergence followed by near-wall divergence on the leeside, was not evident.

The distributions of the eddy viscosity ν_t, and the mixing length ℓ, defined by $-\overline{uv} = \nu_t(\partial U/\partial y) = \ell^2(\partial U/\partial y)^2$, respectively, were also calculated. Cebeci's two-layer eddy-viscosity model, based on a correlation of data in two-dimensional boundary layers, indicates that the maximum value of $\nu_t/U_e\delta_1$, where δ_1 is the displacement thickness, is constant and equal to 0.0168. From the eddy-viscosity data shown in Fig. 10, it is clear that the measurements in the outer part of the boundary layer on the windward side are scattered around this value. The lack of data close to the surface is, however, unfortunate although there is some evidence that the maximum eddy viscosity may be larger than 0.0168. On the other hand, the data on the leeside plane of symmetry indicate

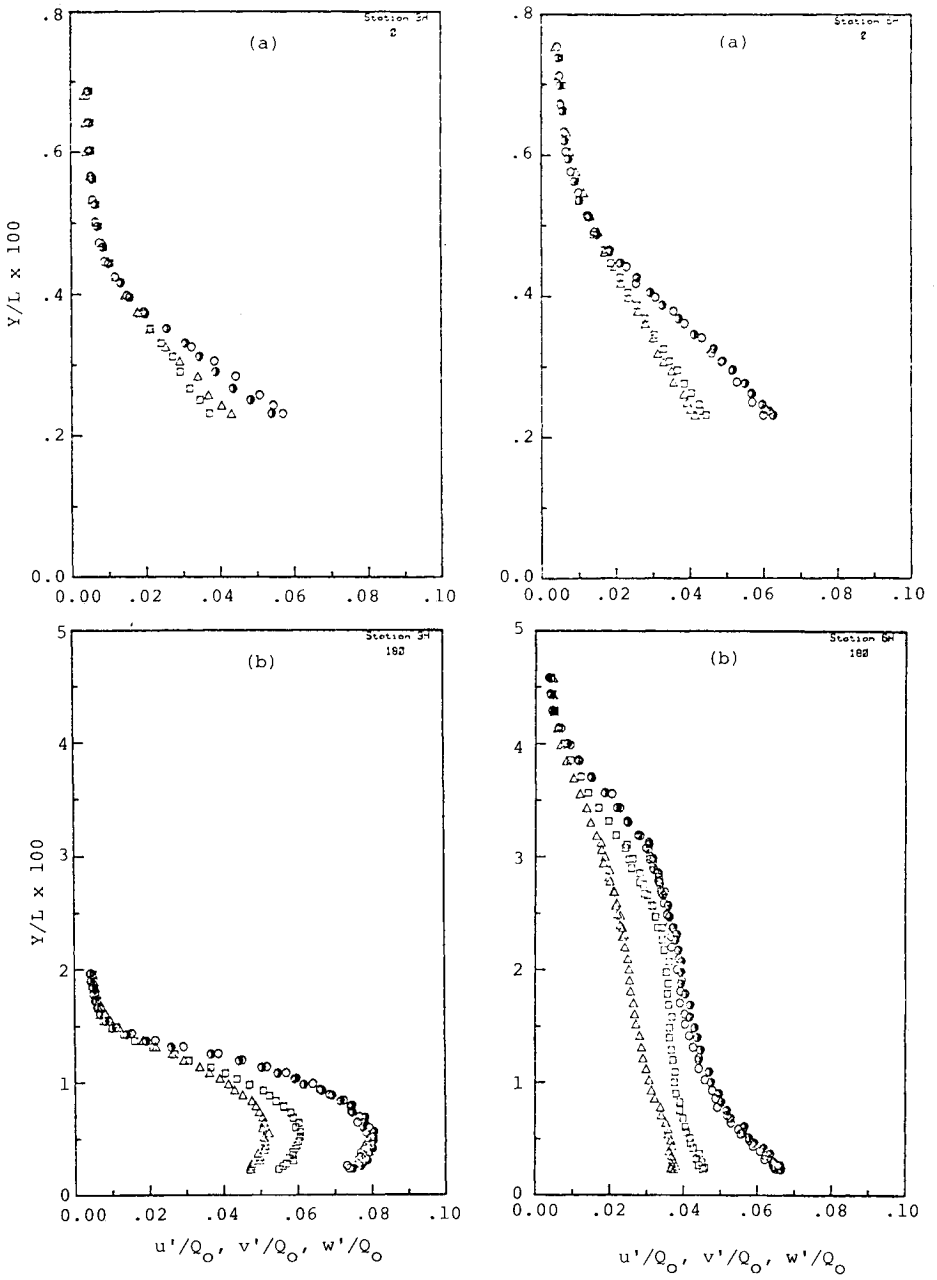

Fig. 7 Turbulence intensities; ○, u' $(u-v)$; ●, u' $(u-w)$; △, v'; □, w': a) windward and b) leeward.

markedly smaller maximum values (of the order of 0.006–0.008). The mixing-length distributions (not shown) indicated trends that are similar and consistent with those of the eddy viscosity. The generally accepted value for ℓ/δ in the outer part of a two-dimensional boundary layer is 0.09. The data on the windward side were again scattered about this value, but those on the leeside indicated a substantial reduction ($\ell/\delta \sim 0.04$–0.05).

In spite of the limitations of the data on the windward side, it appears that there is a significant and consistent effect of mean-flow convergence and divergence on the turbulence-transport properties. The decrease in ν_t and ℓ on the leeside may be attributed to the mean-flow convergence prevailing in the boundary layer over most of the development length up to station 6. Similarly, the divergence of the flow out of the windward plane appears to lead to an increase in these quantities.

With the two hot-wire configurations used, it was possible to measure only seven triple velocity products, namely, $\overline{u^3}$, $\overline{v^3}$, $\overline{w^3}$, $\overline{uv^2}$, $\overline{u^2v}$, $\overline{uw^2}$, and $\overline{u^2w}$. Note that the last of these should be zero by virtue of symmetry. Of the remaining products, i.e., $\overline{vw^2}$, $\overline{v^2w}$, and $\overline{uvw}$, the last two are zero. Thus, all but one ($\overline{vw^2}$) of the nonzero triple products were measured in these experiments.

The data at the two stations on the windward and leeward sides are shown in Figs. 11 and 12. First of all, we note that the distributions of $\overline{u^3}$ measured separately with the two configurations of the probe are in good agreement with each other. This consistency provides some confidence in the data. Second, from Fig. 12 we see that the correlation $\overline{u^2w}$, which should be zero, is not precisely zero everywhere and shows trends similar to those of $\overline{uw}$ discussed earlier. However, it is small relative to the other correlations and, in the thick boundary layer at the leeside station 6H, it is scattered around a zero mean throughout the boundary layer.

Gradients of triple velocity correlations enter the equations controlling the dynamics of the Reynolds stresses through the turbulence diffusion terms, and therefore the data provide information that is of some value in the modeling of turbulence. Diffusion is known to be of important in the inner part of the boundary layer. Unfortunately, the data on the windward side do not extend sufficiently close to the surface to be of more qualitative value. The most that can be said about these data is that the three largest correlations, in the order of decreasing magnitude, are $\overline{u^3}$, $\overline{u^2v}$, and $\overline{uv^2}$. This is not particularly surprising in view of the relative magnitudes of the turbulence components u' and v'. Although $\overline{u^3}$ is large, its longitudinal derivative, which represents the diffusion of

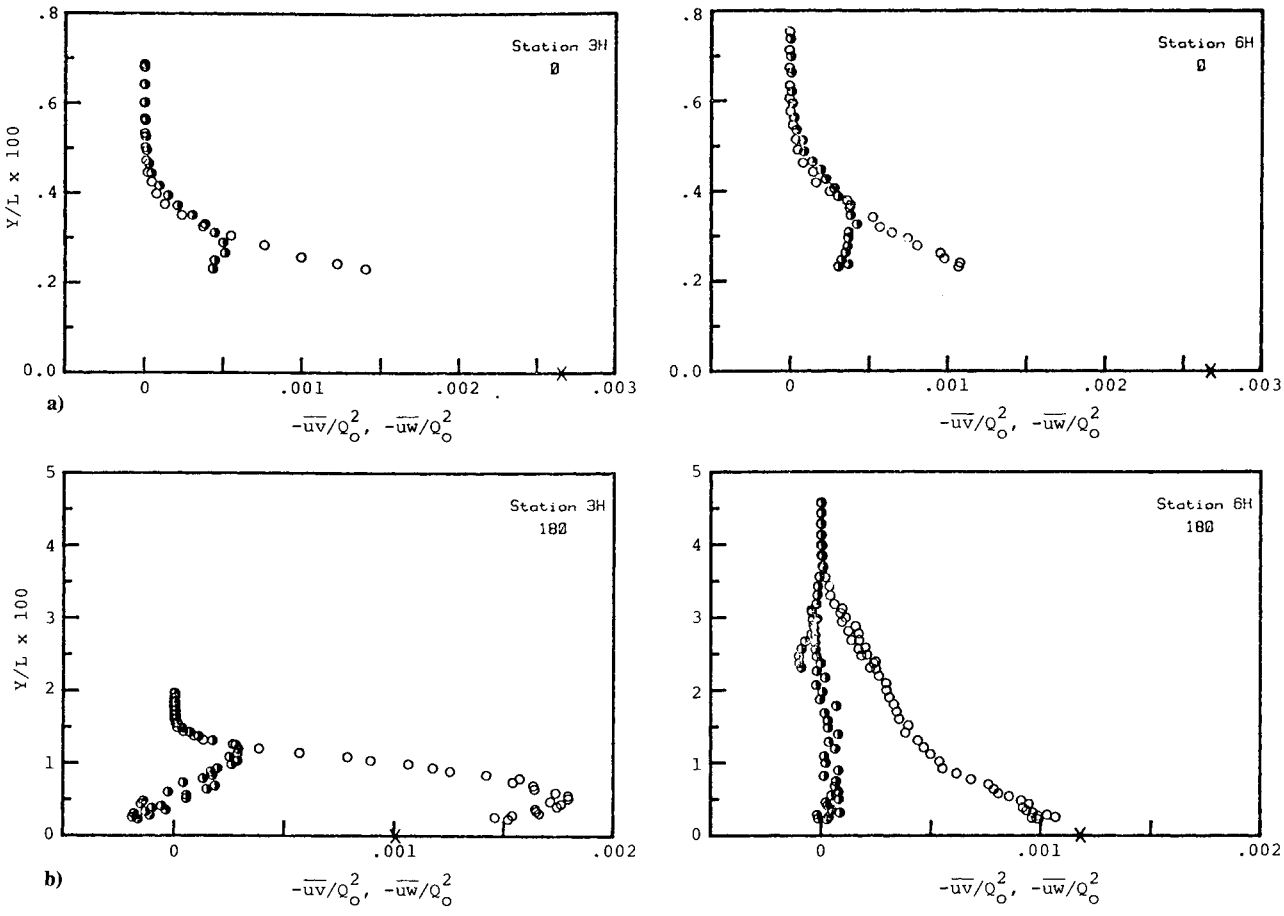

Fig. 8 Shear stresses; ○, $\overline{uv}$; ●, $\overline{uw}$; x, wall shear (from velocity profiles): a) windward and b) leeward.

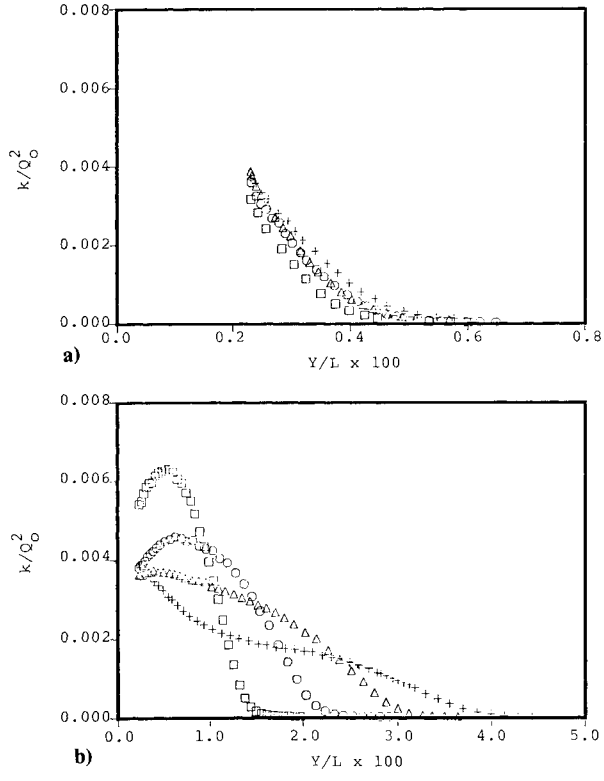

Fig. 9 Turbulent kinetic energy k. □, 3H; ⬡, 4H; △, 5H; +, 6H: a) windward and b) leeward.

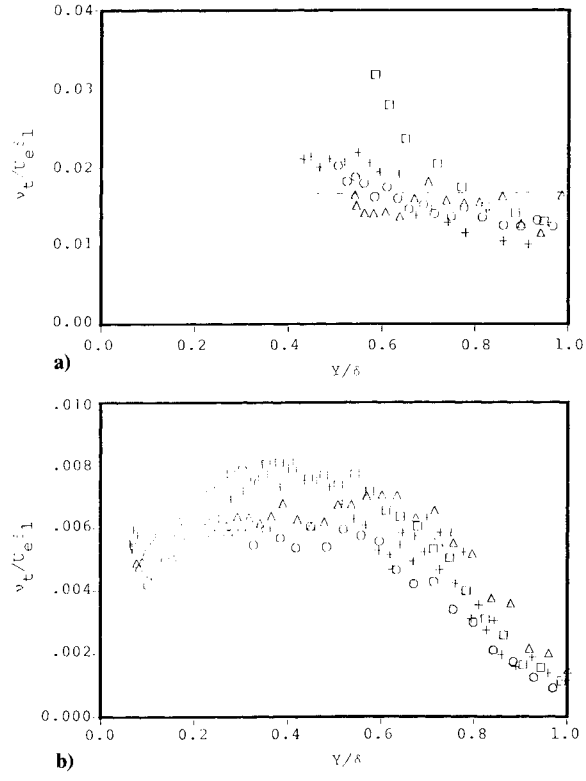

Fig. 10 Eddy-viscosity profiles; symbols as in Fig. 9: a) windward and b) leeward.

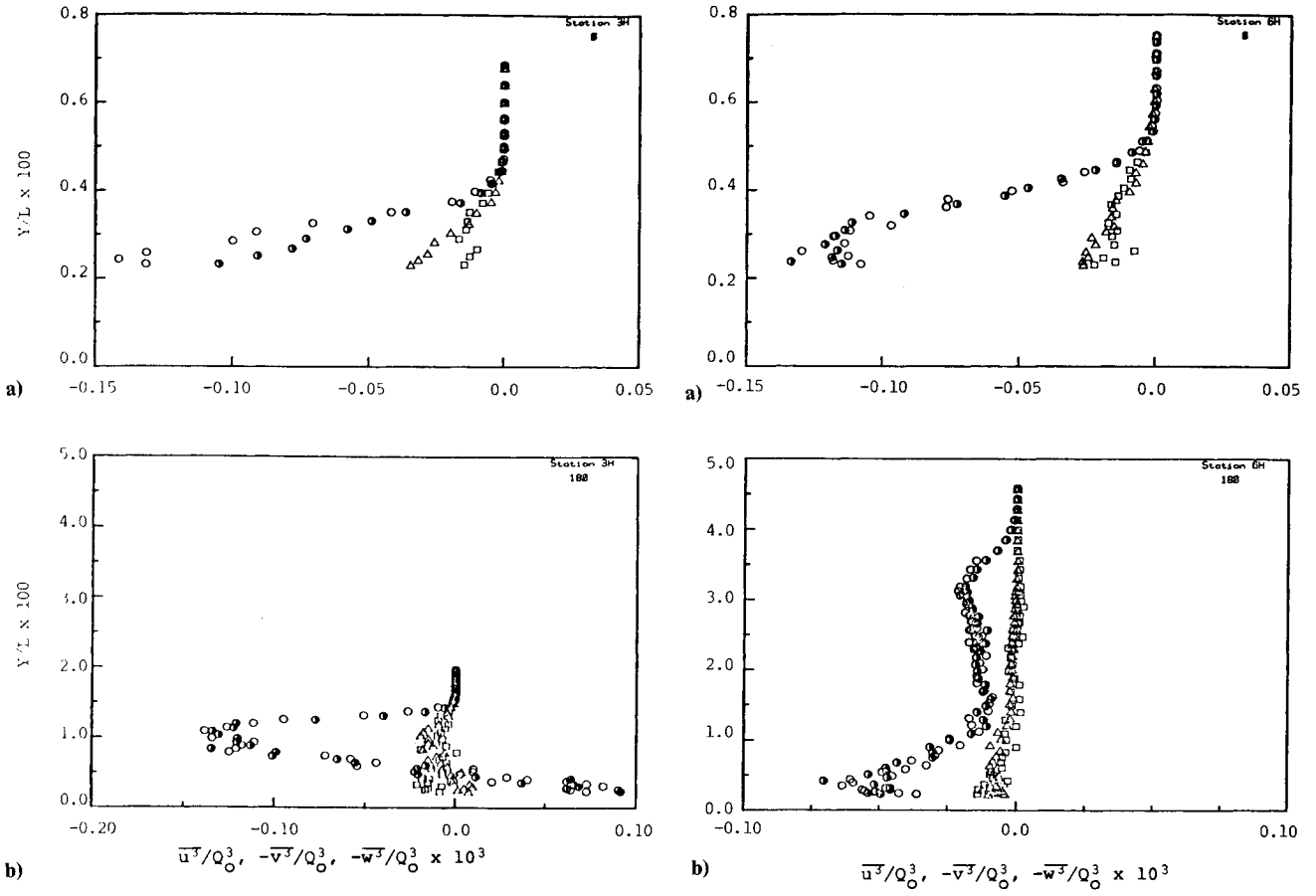

Fig. 11 Triple correlations; ○, $\overline{u^3}$ $(u-v)$; ⊙, $\overline{u^3}$ $(u-w)$; Δ, $\overline{v^3}$; □, $\overline{w^3}$: a) windward and b) leeward.

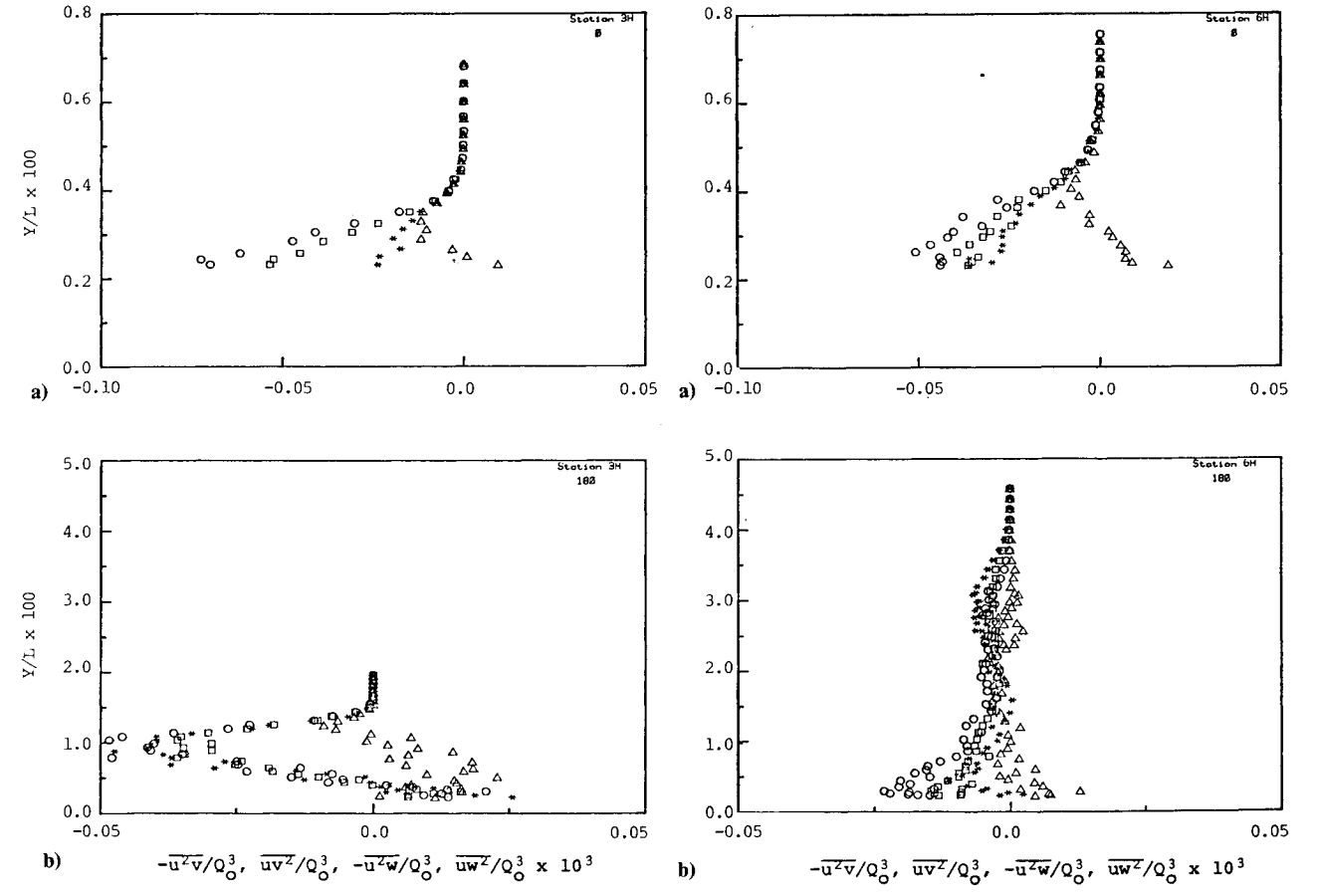

Fig. 12 Triple correlations; ○, $\overline{u^2v}$; □, $\overline{uv^2}$; Δ, $\overline{u^2w}$; *, $\overline{uw^2}$: a) windward and b) leeward.

$\overline{u^2}$, is usually neglected within boundary-layer approximations. The normal derivatives of $\overline{u^2v}$ and $\overline{uv^2}$ account for the diffusion of $\overline{u^2}$ and $\overline{uv}$, respectively, which are the two primary Reynolds stresses. In spite of their obvious limitations, the data on the windward side have been presented here for completeness.

On the leeside, the relative magnitudes of the triple correlations are similar to those on the windward side. At the upstream station, the trends in the outer part of the boundary layer are in fact the same as those on the windward side. The large negative gradients of $\overline{u^2v}$ and $\overline{uv^2}$ observed in the wall region at this station indicate a loss of $\overline{u^2}$ and $\overline{uv}$, respectively, due to turbulent diffusion. This is in accordance with measurements in two-dimensional boundary layers. However, these gradients become quite small downstream and, at station 6H, their sign is reversed, indicating quite a different behavior of turbulent diffusion. The data at station 6H are particularly noteworthy since we see a large region in the outer part of the boundary layer where all triple correlations are very small and an inner region where their gradients are significant but opposite to those seen further upstream and in two-dimensional boundary layers. This is presumably due to the development of the local region of mean-flow divergence which, as shown in Fig. 6, leads to a large negative normal component of mean velocity. Although the evidence is rather limited, the data suggest a significant influence of the extra strain rates due to mean-flow divergence on the diffusive mechanism. The lack of similar data in the wall region of the windward boundary layer, which experiences continuous flow divergence, is unfortunate since such data would have provided confirmation of this conclusion.

VI. Conclusions

Mean-flow and turbulence measurements in the boundary layer in the planes of symmetry of a body of revolution at incidence have been described. Although the rather thin boundary layer on the windward side precluded detailed turbulence measurements in the wall region, the data indicate a direct effect of flow divergence and convergence on the turbulence structure. The available evidence suggests that prolonged convergence leads to a region of flow divergence in the inner part of the boundary layer and a reduction in the turbulence level. The latter feature is also reflected in a significant decrease in the eddy viscosity and mixing length.

The data presented here are used, along with some previous results, in a parallel computational study to clarify further the effects of convergence and divergence on the mean flow and turbulence. This is reported in Part II.[1]

Acknowledgments

This research was supported by the U.S. Army Research Office and U.S. Air Force Office of Scientific Research under Grant AFOSR-80-0148B.

References

[1]Patel, V.C. and Baek, J.H., "Boundary Layers in Planes of Symmetry. Part II: Calculations for Laminar and Turbulent Flows," *AIAA Journal,* (to be published).

[2]Wang, K.C., "Three-Dimensional Boundary Layer near the Plane of Symmetry of a Spheroid at Incidence," *Journal of Fluid Mechanics,* Vol. 43, 1969, pp. 187–209.

[3]Wang, K.C., "Laminar Boundary Layer near the Symmetry Plane of a Prolate Spheroid," *AIAA Journal,* Vol. 12, Dec. 1974, pp. 949–958.

[4]Schneider, G.R., "Calculation of Three-Dimensional Boundary Layers in the Plane of Symmetry of a Prolate Spheroid at Incidence Including the Laminar-Turbulent Transition," *Proceedings of the 8th USAF-FRG Data Exchange Agreement Meeting,* Gottingen, FRG, May 1983.

[5]Meier, H.U. and Kreplin, H.P., "Experimental Investigation of Boundary Layer Transition and Separation on a Body of Revolution," *Zeitschrift für Flugwiss Weltraumforschung,* Vol. 4, 1980, pp. 65–71.

[6]Kreplin, H.P., Vollmers, H., and Meier, H.U., "Experimental Determination of Wall Shear Stress Vectors on an Inclined Prolate Spheroid," *Proceedings of the 5th USAF-FRG Data Exchange Agreement Meeting,* AFFDL-TR-80-3088, 1980, pp. 315–332.

[7]Meier, H.U., Kreplin, H.P., and Vollmers, H., "Velocity Distributions in 3-D Boundary Layers and Vortex Flows on an Inclined Prolate Spheroid," *Proceedings of the 6th USAF-FRG Data Exchange Agreement Meeting,* DFVLR – AVA Rept. IB 22281 CP1, 1981, pp. 202–217.

[8]Kreplin, H.P., Vollmers, H., Meier, H.U., "Measurements of the Wall Shear Stress on an Inclined Prolate Spheroid," *Zeitschrift für Flugwiss Weltraumforschung,* Vol. 6, 1982, pp. 248–252.

[9]Hornung, H.G. and Joubert, P.N., "The Mean Velocity Profile in Three-Dimensional Turbulent Boundary Layers," *Journal of Fluid Mechanics,* Vol. 15, 1963, pp. 368–385.

[10]East, L.F. and Hoxey, R. P., "Low-speed Three-Dimensional Turbulent Boundary Layer Data. Part 1," *British Aeronautical Research Council,* R&M 3653, 1969.

[11]Dechow, R. and Felsch, K.O., "Measurements of the Mean Velocity and of the Reynolds Stress Tensor in a Three-Dimensional Turbulent Boundary Layer Induced by a Cylinder Standing on a Flat Wall," *Proceedings of the 1st Symposium on Turbulent Shear Flows,* Pennsylvania State Univ., University Park, PA, 1977, pp. 9.11–9.20.

[12]Krogstad, P.A., "Investigation of a Three-dimensional Turbulent Boundary Layer Driven by Simple Two-Dimensional Potential Flow," Dr. Ing. Thesis, Norwegian Institute of Technology, Trondheim, Norway, 1979.

[13]Pierce, F.J. and McAllister, J.E., "Near-Wall Similarity in a Pressure-Driven Three-Dimensional Turbulent Boundary Layer," Virginia Polytechnic Inst. and State Univ., Rept. VPI-E-80.32, 1980.

[14]Ramaprian, B.R., Patel, V.C., and Choi, D.H., "Mean Flow Measurements in the Three-Dimensional Boundary Layer over a Body of Revolution at Incidence," *Journal of Fluid Mechanics,* Vol. 103, 1981, pp. 479–504.

[15]Bradshaw, P., "Effects of Streamline Curvature on Turbulent Flow," AGARDograph No. 169, 1973.

[16]Landweber, L. and Macagno, M., "Irrotational Flow about Ship Forms," Iowa Institute of Hydraulic Research, Univ. of Iowa, Iowa City, IIHR Rept. 123, 1969.

[17]Baek, J.H. and Patel, V.C., "Laminar and Turbulent Boundary Layers in a Plane of Symmetry," Iowa Institute of Hydraulic Research, Univ. of Iowa, Iowa City, IIHR Rept. 278, 1984.